Macromolecules

pubs.acs.org/Macromolecules
Article

Introducing Dimethyl Ether as a Solvent for Anionic Polymerization: Comprehensive Kinetics of Dienes and Styrene

Frédéric S. Petrov, Manfred Wagner, Holger Frey,* and Axel H. E. Müller*

Cite This: *Macromolecules* 2026, 59, 8274–8284
Read Online

ABSTRACT: This work aims to shed light on the use of the highly available, yet unexplored dimethyl ether (DME) as a solvent for anionic polymerizations. DME is virtually nontoxic and does not lead to the formation of peroxides. The development of special techniques and setups, for the first time, enabled the use of liquid DME, exhibiting a vapor pressure of 6 bar at 25 °C, as a (co)solvent for the anionic polymerization of isoprene (I), β-myrcene (Myr), β-farnesene (Far), and styrene (S) using *sec*-butyllithium as an initiator. Propagation constants, kinetic orders, and activation energies of I, Myr, and Far in DME were determined at 0, 10, and 23 °C using in situ ^{1}H NMR kinetics. The use of DME leads to faster monomer consumption compared to the less polar methyl *tert*-butyl ether (MTBE). Additionally, the effect of increasing amounts of DME on the reactivity ratios of S/I copolymerizations up to [DME]/[Li] = 450 in cyclohexane (CHx) was investigated using in situ near-infrared (NIR) spectroscopy. The necessary amount of polar ether modifier to reach random (i.e., $r_I \approx r_S \approx 1$) S/I incorporation inversely correlates with the polarity of the solvent, i.e., MTBE < DME < THF. Using in situ ^{1}H NMR kinetics, the same trend could be established for the stability toward *n*-butyllithium in the respective ethers. NIR kinetics revealed that the polymerization rate of styrene in CHx at 20 °C is accelerated ≈18 times at [DME]/[Li] = 30. Lastly, the effect of Li, Na, K, Rb, and Cs naphthalenides on the microstructure of polyisoprene (PI) synthesized in DME at room temperature was determined and found to be comparable to PI synthesized in 1,4-dioxane.

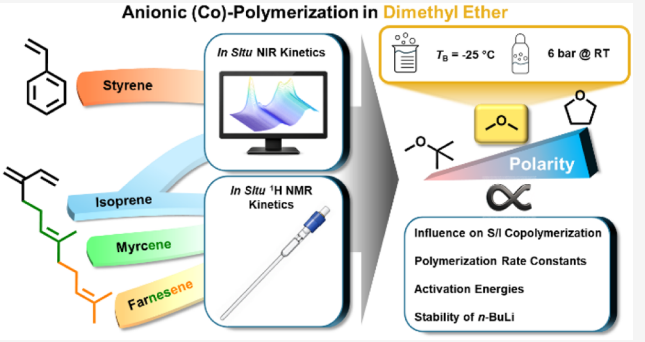

INTRODUCTION

Anionic polymerization of vinyl monomers in aprotic solvents such as cyclohexane (CHx), benzene, toluene, tetrahydrofuran (THF), and 1,2-dimethoxyethane has been studied extensively. Hydrocarbon solvents in combination with alkyllithium initiators such as *sec*-butyllithium (*sec*-BuLi) are favored because of their ability to polymerize 1,3-dienes like 1,3-butadiene or isoprene (I) in a 1,4-manner, yielding polymers exhibiting a low glass transition temperature, T_g, which is desired for many industrially relevant copolymers.[1] Besides hydrocarbons,[2−5] ethers like THF,[6−13] methyl *tert*-butyl ether (MTBE),[14−16] cyclopropyl methyl ether,[17−20] 2- or 3-methyltetrahydrofuran,[17,21] diethyl ether,[6,8,22] tetrahydropyran,[13,23,24] diisopropyl ether,[7] diphenyl ether,[7,25] anisole,[7,25−27] 1,4-dioxane,[7,8,12,28,29] 1,2-dimethoxyethane,[10,21,30,31] triethylene glycol dimethyl ether,[32] 2,2-di(2-tetrahydrofuryl)-propane,[33,34] and amines like trialkylamines[7] and *N*,*N*-dimethylaniline[7] have also been used as (co)solvents to polymerize vinylic monomers and 1,3-dienes.

However, to the best of our knowledge, there is no published literature on the use of dimethyl ether (DME) for anionic polymerizations. DME exhibits a boiling point of T_b = −25 °C and a vapor pressure of 6 bar at 25 °C (Figure S16).[35,36]

While there are many reports either describing DME as a solvent for extractions[38,39] or as an alternative for conventional diesel or liquefied petroleum gas,[40,41] there is only a handful of publications in the whole field of chemistry which report on the usage of DME as a solvent for chemical reactions.[37,42−51] For example, radical dispersion polymerizations were conducted in compressed DME as an alternative to supercritical CO_2.[44−46]

DME is also used as a refrigerant,[52] as a propellant in aerosol products,[52] and in the production of dimethyl sulfate.[35] It is worth noting that DME is virtually nontoxic[53] and does not lead to the formation of peroxides.[54−56] DME can be obtained by direct synthesis from synthesis gas (CO + H_2)[57] or from the dehydration of methanol,[35] which itself can potentially be sourced via the hydrogenation of CO_2[58] or from biomass.[59]

Received: May 8, 2026
Revised: June 24, 2026
Accepted: June 30, 2026
Published: July 16, 2026

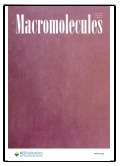

https://doi.org/10.1021/acs.macromol.6c01289
Macromolecules 2026, 59, 8274−8284

Ethers, being Lewis bases, solvate the counterions and therefore increase the nucleophilicity of the active chain ends. Hence, compared to nonpolar solvents, the use of ethers generally leads to faster consumption of monomers in anionic polymerizations.[60,61] In hydrocarbon solvents, the active chain ends of polymers form aggregates.[62−64] Using light-scattering measurements, a 4-fold association of polyisoprenyl-Li was found, which correlates with a determined kinetic order, *N*, of one-quarter.[64] On the one hand, polar solvents like ethers lead to a shift of the aggregation-disaggregation equilibrium of chain ends toward the active, nonaggregated species.[64,65] For example, it is generally accepted that the degree of association is unity for polymerizations of butadiene, isoprene, and styrene (S) in THF.[65−67] On the other hand, the dissociation of ion pairs into free anions increases with increasing polarity of the solvent.[68]

The use of ethers as solvents for anionic polymerizations is accompanied by chain termination reactions due to ether cleavage by active alkyllithium species.[15,69−73] The rate of degradation depends on the ether,[15] the counterion[72,74] and the substituent.[73,75,76] For example, it was found recently that the half-life of *n*-BuLi in MTBE at 20 °C is ≈ 2600 min, whereas in THF it is ≈ 44 min.[15] It is worth noting that an autocatalytic degradation was observed in MTBE, while the degradation of *n*-BuLi in THF obeyed first-order kinetics. More polar solvents exhibit stronger solvating power, as quantified by the dielectric constant, ε, and hence have a larger influence on the rate of anionic polymerizations.[15,34,77] For example, whereas S/I copolymerizations in pure CHx lead to tapered block copolymers favoring the initial incorporation of isoprene, the addition of ≈ 6 equivalents (equiv) THF (ε^{THF} = 7.52)[78] relative to *sec*-BuLi as a modifier leads to random incorporation of both monomers ($r_S \approx r_I \approx 1$), whereas ≈ 166 equiv MTBE (ε^{MTBE} = 2.6)[79] are required to achieve the same outcome.[15,77] Liquid DME, exhibiting an intermediate dielectric constant of ε^{DME} = 5.034 at 24.5 °C,[80] can be used as a solvent for the quantitative reaction of sodium with naphthalene, yielding sodium naphthalenide (Na-Naph), which is also achievable in THF but not in MTBE.[42]

Due to its volatile nature (boiling point of −25 °C), in this work, special techniques and setups had to be developed to dry DME and use it as a (co)solvent for *sec*-BuLi-initiated anionic polymerizations. Using in situ ^{1}H NMR measurements, the stability of DME against alkyllithium compounds, as well as the polymerization kinetics of isoprene, *β*-myrcene (Myr), and *β*-farnesene (Far) polymerization in DME, was investigated. The effect of increasing amounts of DME as an additive in CHx on the homopolymerization kinetics of styrene and on copolymerizations of styrene and isoprene was studied using in situ near-infrared (NIR) spectroscopy. Lastly, the effect of alkali cations on the microstructure of polyisoprene synthesized in DME was examined.

RESULTS AND DISCUSSION

Stability of DME against *n*-Butyllithium

To investigate the stability of DME toward organolithium compounds, excess DME and *n*-BuLi were transferred into a pressure-resistant NMR tube, and the decrease of the −CH_2−Li protons was tracked via in situ ^{1}H NMR spectroscopy at 20 °C (Figure S23). Details regarding the drying and handling of DME are given in the Supporting Information, Section 1.3 and Section 1.4, respectively. Figure 1 shows the decrease of [*n*-BuLi] as well as the corresponding pseudo first-order plot according to eq 1.

$$\ln\left(\frac{[\mathrm{BuLi}]_0}{[\mathrm{BuLi}]}\right) = k_{deg}t \quad (1)$$

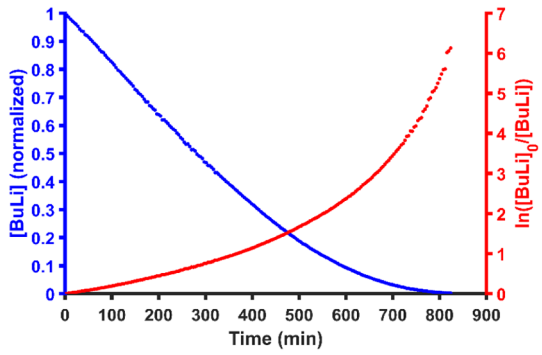

Figure 1. Decrease of *n*-BuLi concentration at 20 °C (blue) and pseudo first-order plot (red) tracked using in situ ^{1}H NMR kinetics.

Similar to the observation in MTBE,[15] the slope of the pseudo first-order plot, which corresponds to the hypothetical first-order degradation rate constant k_{deg}, shows an upward curvature, indicating an autocatalyzed degradation of *n*-BuLi. Ziegler et al. reported that besides the formation of LiOMe, higher alkanes (C ≥ 4) are formed during the degradation of *n*-BuLi in DME (Scheme 1).[37] This was explained by the successive in situ insertion of methylene groups into *n*-BuLi. It was reported that *n*-BuLi in THF at 22 °C is at least trimeric.[81] We assume that this is also true for *n*-BuLi in DME. Furthermore, we assume that the in situ formed higher *n*-alkyllithium compounds aggregate to a lesser extent and therefore lead to a faster degradation reaction. The half-life of the degradation of the initial *n*-BuLi concentration, $[\mathrm{BuLi}]_0$, in DME is $t_{1/2}^{DME} \approx$ 280 min, whereas in MTBE the half-life of $[\mathrm{BuLi}]_0$ is about 1 order of magnitude larger with $t_{1/2}^{MTBE} \approx$ 2600 min.[15] It should be noted again that both reactions are autocatalyzed, whereas in THF the degradation obeys first-order kinetics with a constant half-life of $t_{1/2,const.}^{THF} \approx$ 44 min.[15] Nonetheless, it can be stated that the rate of degradation follows the polarity of the solvent, i.e., MTBE < DME < THF. This could be explained by a favored deaggregation of *n*-BuLi by more polar solvents, which would accelerate the decomposition reaction.

Kinetics of Isoprene, *β*-Myrcene, and *β*-Farnesene Polymerization in DME

To gauge the effect of DME on the polymerization of established dienes in situ, ^{1}H NMR kinetic experiments were conducted (see Figures S24-S26 for representative stacked ^{1}H NMR spectra). In this work, the concentration of active chain ends, [P*], was calculated according to eq 2, which involves the molecular weight of the respective monomer, M_M, the initial monomer concentration, $[M]_0$, and the determined molecular weight, M_n^{SEC}, using size exclusion chromatography (SEC), with a PI calibration.

$$[P^*] = \frac{[M]_0 M_M}{M_n^{SEC}} \quad (2)$$

Due to overlapping signals, ^{1}H NMR was not used to calculate the corresponding M_n^{NMR} values (Figures S28−S29).

https://doi.org/10.1021/acs.macromol.6c01289
Macromolecules 2026, 59, 8274−8284

Scheme 1. Decomposition Reaction of DME in the Presence of *n*-BuLi Proposed by Ziegler et al.[37]

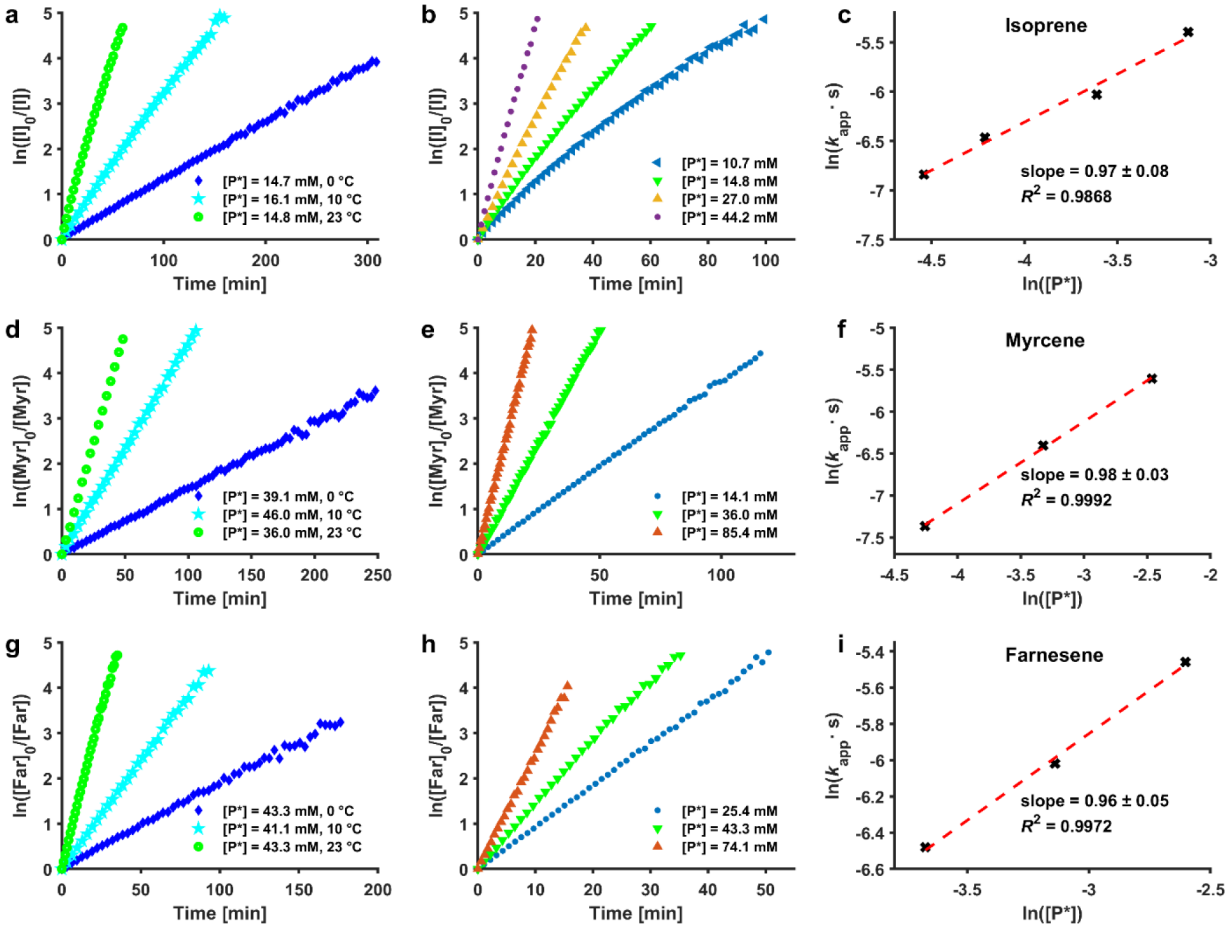

Figure 2. Results of in situ ^{1}H NMR kinetics of isoprene (a–c), myrcene (d,f), and *β*-farnesene (g–i) in DME using *sec*-BuLi as initiator. (a,d,g) Pseudo first-order plots at different temperatures at comparable concentrations of polymer chains [P*]. (b,e,h) Pseudo first-order plots for different [P*] at 23 °C. (c,f,i) Kinetic order plots for polymerizations shown in (b),(e),(h) according to eq 4. Note: When the pseudo first-order plot showed a downward curvature, the initial slope was used to determine k_{app} (see Supporting Information, Figure S30).

Figure 2 shows pseudo first-order plots and kinetic order plots for polymerizations of I, Myr, and Far in DME.

All three monomers were polymerized at three different temperatures, 0 °C, 10 °C, and 23 °C, using comparable concentrations of initiator (Figure 2a,d,g). Additionally, for each monomer, multiple polymerizations using different amounts of initiator were conducted at 23 °C (Figure 2b,e,h). Full conversion was reached for all experiments (Figure S27), and the kinetic data are summarized in Table 1. In the case of a living polymerization, the pseudo first-order plot is linear, and the slope yields k_{app}.[82] The propagation rate constant, k_p, is calculated using eq 3.

$$k_p = \frac{k_{app}}{[P^*]^N} \tag{3}$$

It should be stressed that if the kinetic order, N, with respect to [P*], is below unity, k_p is dependent on the equilibrium constant between inactive, aggregated polymer chains and active unimers.[83] Linearization of eq 3 leads to eq 4, which can be used to construct a double logarithmic plot of the apparent rate constant k_{app} against [P*] to determine N.

$$\ln(k_{app}) = N \cdot \ln([P^*]) + \ln(k_p) \tag{4}$$

Recently, $N \approx 1$ was found for isoprene and farnesene, initiated by *sec*-BuLi in MTBE at 23 °C.[15] As expected, for polymerizations of I, Myr, and Far in the more polar DME at 23 °C, N was also found to be unity (Figure 2c,f,i). According to the prevailing interpretation for the use of nonpolar to moderately polar solvents, this corresponds to a degree of association of $n_{Agg} = 1/N \approx 1$.[64,84] Furthermore, the observation of $N \approx 1$ can be interpreted as the absence of an equilibrium between polydienyl-Li ion pairs and free polydienyl anions.[85] Hence, it can be assumed that the determined k_p values in DME correspond to the propagation constant of the ion-pairs. If the respective solvent has a rather high dielectric constant, then the tendency to coordinate lithium is expected to be increased. Therefore, the interionic distance to the negatively charged polymer chains should increase, leading to a higher reactivity of the propagating chain ends. Hence, for a given monomer, one expects to observe increasing rates of polymerization and decreasing activation energies with increasing polarity of the solvent, i.e., MTBE <

https://doi.org/10.1021/acs.macromol.6c01289
Macromolecules 2026, 59, 8274–8284

Table 1. Overview of Kinetic Parameters of Isoprene, Myrcene, and β-Farnesene in DME Using *Sec*-BuLi and Corresponding Polymer Microstructure, Molecular Weight, and Glass Transition Temperature

Exp.	T (°C)	[P*][a] (mmol L^{-1})	k_{app}[b] (10^{-3} s^{-1})	k_p[c] (10^{-3} M^{-1} s^{-1})	M_n^{SEC}[d] (kg mol^{-1})	$Đ$[d]	1,4-[e] (%)	3,4-[e] (%)	1,2-[e] (%)	T_g[f] (°C)
Isoprene										
Iso1	0	14.7	0.23	15.6	7.3	1.10	6.9	71.6	21.5	13
Iso2	10	16.1	0.57	35.4	6.0	1.10	9.1	69.8	21.1	13
Iso3	23	14.8	1.55	105	10.0	1.04	10.3	69.4	20.3	12
Iso4	23	27.0	2.41	89.3	4.8	1.11	10	70.2	19.8	-
Iso5	23	10.7	1.07	100	9.9	1.05	11.1	68.5	20.4	8
Iso6	23	44.2	4.53	102	3.5	1.07	10.4	69.7	19.9	5
Myrcene										
Myr1	0	39.9	0.24	6.0	3.3	1.13	24.4	66.2	9.4	−48
Myr2	10	46.0	0.78	17.0	3.5	1.12	26.4	65.4	8.2	−48
Myr3	23	36.0	1.65	45.8	3.7	1.12	29.3	64.1	6.6	−49
Myr4	23	85.4	3.67	43.0	1.9	1.16	30.1	63.6	6.3	−57
Myr5	23	14.1	0.63	44.8	10.3	1.04	27.9	65.2	6.9	−44
Farnesene										
Far1	0	43.3	0.31	7.21	3.7	1.15	24.2	66.6	9.2	−68
Far2	10	41.1	0.79	19.2	3.9	1.15	26.8	65.4	7.8	−68
Far3	23	43.3	2.42	59.0	3.7	1.14	28.3	65.0	6.7	−68
Far4	23	74.1	4.26	57.5	2.6	1.14	29.5	62.9	7.6	−70
Far5	23	25.4	1.56	61.4	7.5	1.07	28.8	64.1	7.1	−67

[a]Concentration of polymer chains, [P*] = $[M]_0 M_M/M_n^{SEC}$ (M_M: molar mass of monomer). [b](Initial) slope of pseudo first-order plot (Figure 2). [c]Polymerization rate constant, $k_p = k_{app}/[P^*]^N$ (assuming $N = 1$). [d]Determined by SEC (calibration: PI, eluent: THF). [e]Determined via ^{1}H NMR spectroscopy. [f]Determined via DSC (second heating curve was used for evaluation, heating rate: 10 K min^{-1}). For SEC and DSC curves, see Figures S31−S36.

DME < THF.[21] Indeed, the k_p value of isoprene in DME at 23 °C is about seven times higher as compared to MTBE, whereas for farnesene, it is about three times higher (Table 2).[15]

Table 2. Polymerization Rate Constants k_p at 23 °C and Activation Energies E_A for I, Myr, and Far (Li Counterion)

Monomer	Solvent	k_p (10^{-3} M^{-1} s^{-1})	E_A (kJ mol^{-1})
Isoprene	THF[a]	134	42
Isoprene	DME	99 ± 6[b]	53 ± 0
Isoprene	MTBE[c]	13	66 ± 2
Myrcene	DME	45 ± 1[d]	58 ± 5
Farnesene	DME	59 ± 2[e]	61 ± 1
Farnesene	MTBE[c]	23	70 ± 0

[a]Values taken from Garton et al. (extrapolated k_p).[87] [b]Average value of Iso3−Iso6. [c]Values taken from Meier-Merziger et al.[15] [d]Average value of Myr3−Myr5. [e]Average value of Far3−Far5.

Interestingly, whereas in both CHx and MTBE the k_p values for farnesene are higher than for isoprene,[3,15,86] the inverse trend is observed in DME. The higher polarity of DME seems to facilitate the incorporation of the comparatively small isoprene monomer, whereas the addition of the bulkier myrcene and farnesene monomers is less likely. Also, the extrapolated value of $k_p = 134 \cdot 10^{-3}$ M^{-1} s^{-1} for polyisoprenyl-Li ion pairs in the more polar THF at 23 °C, as reported by Garton et al.,[87] is higher than the propagation constant of ion-pairs in DME at 23 °C ($k_p = 99.1 \cdot 10^{-3}$ M^{-1} s^{-1}, Table 2).

In contrast to the linear pseudo first-order plots of myrcene and farnesene (Figures 2e and 2h, respectively), a downward curvature was obtained for polymerizations of isoprene in DME at 23 °C, indicating the presence of chain termination reactions (Figure 2b). The data can be readily described by a kinetic model, which considers a pseudo first-order termination reaction of polyisoprenyl-Li with DME (eq S10, Figure S30). As can be expected, the extent of chain termination reactions, as quantified by the termination constant, k_t, decreases from $k_t \approx 139 \cdot 10^{-7}$ M^{-1} s^{-1} at 23 °C to $k_t \approx 6 \cdot 10^{-7}$ M^{-1} s^{-1} at 0 °C (Table S1). Proton abstractions from DME by the polyisoprenyl anion could account for the good fit of the pseudo first-order termination model. Additionally, slow elimination of lithium hydride from the active centers, followed by a fast proton abstraction of the subsequently formed conjugated system, as postulated by Szwarc and coworkers for polystyryl sodium,[88] yielding a highly delocalized heptatrienyl anion, would also be a first-order process. However, since Garton et al. found no evidence for the transformation of polyisoprenyl-Li in THF to such a delocalized anion,[87] we assume, in analogy to the reaction of *n*-butyllithium with DME,[37] that ongoing proton abstractions from DME by the highly basic polyisoprenyl anion lead to the termination of the growing chain. Apparently, the nucleophilicity of polyisoprenyl-Li compared to that of polymyrcenyl-Li and polyfarnesyl-Li in DME is enhanced, which leads to the highest reactivity toward diene incorporation but also toward termination reactions. An explanation for the occurrence of termination reactions of polyisoprenyl-Li is given further below. A similar characteristic difference between isoprene on the one hand and myrcene and farnesene on the other hand can be seen in the activation energies and the polydiene microstructures (see below).

Determination of Activation Energies

The propagation rate constants, k_p, of polymerizations conducted at different temperatures were plotted using the linearized Arrhenius equation (eq 5) and are shown in Figure 3.

$$\ln(k_p) = \ln(A) - \frac{E_A}{R} \cdot \frac{1}{T} \quad (5)$$

E_A is the activation energy, R is the universal gas constant, and T is the absolute temperature.

https://doi.org/10.1021/acs.macromol.6c01289
Macromolecules 2026, 59, 8274−8284

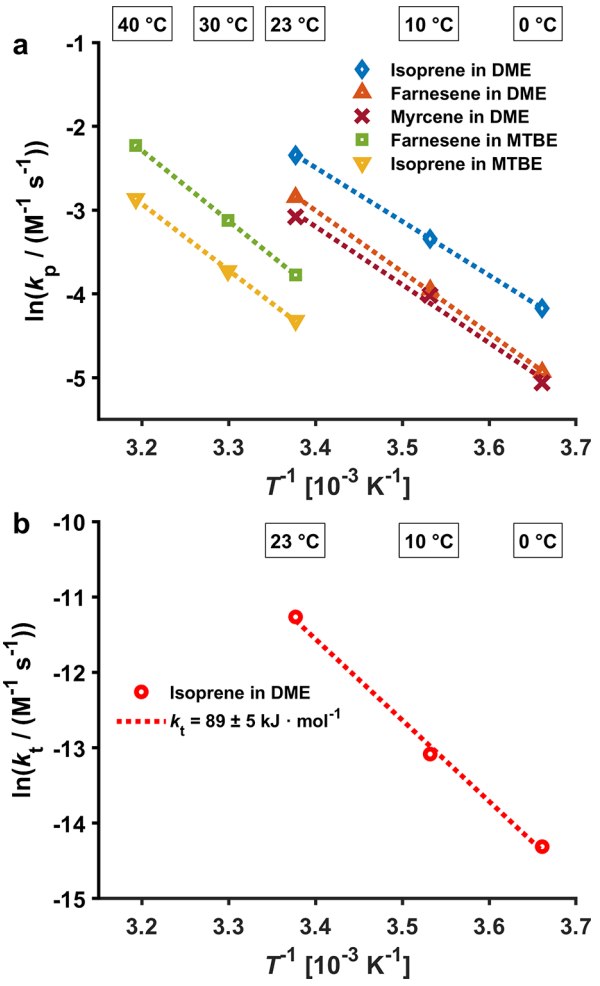

Figure 3. (a) Arrhenius plots of the propagation reactions of isoprene, myrcene, and farnesene in DME and of isoprene and farnesene in MTBE. (b) Arrhenius plot of the pseudo first-order termination reaction of polyisoprenyl-Li with DME. Data for polymerizations in MTBE were taken from Meier-Merziger et al.[15] Copyright 2024 American Chemical Society.

Compared to MTBE, E_A values in DME for isoprene and farnesene are ≈ 13 and ≈ 9 kJ mol^{-1} lower, respectively (Table 2).[15] This is in agreement with the faster propagation in DME. Evidently, compared to MTBE, DME leads to better stabilization of the transition state. Following the polarity of the solvents, the reported activation energy for the propagation of polyisoprenyl-Li ion pairs in THF is ≈ 12 kJ mol^{-1} lower than in DME.[87]

Also, the E_A values for myrcene and farnesene in DME lie in a similar range of ≈ 58 − 61 kJ mol^{-1}, whereas isoprene exhibits a lower value of ≈ 53 kJ mol^{-1}. Similarly, the E_A value for the pseudo first-order termination reaction of polyisoprenyl-Li with DME was calculated to be at 89 ± 5 kJ mol^{-1}. This relatively high value reflects the observation that full conversion was reached in each case despite the presence of chain termination reactions.

Microstructures and Glass Temperature

The determination of the polydiene microstructures is detailed in the Supporting Information, Section 4.4. As shown in Table 1, the microstructures of PMyr and PFar in DME do not differ significantly (1,4-/3,4-/1,2-units ≈ 28/65/7), whereas PI exhibits significantly more 1,2-units and fewer 1,4-units (1,4-/3,4-/1,2-units ≈ 10/70/20). In principle, two different dienyl anions can form upon the addition of a 2-substituted 1,3-diene to a carbanion (dienyl (I) and dienyl (II), Figure 4). As evidenced by the amount of 1,2-units, nucleophilic addition to the 1-position of the respective diene, resulting in dienyl (I), is increased for isoprene compared to the other two dienes, yielding a delocalized carbanion with a rather nucleophilic carbon at the former 4-position due to (i) the inductive effect of the two substituents at the former 2-position and (ii) the absence of a substituent at the adjacent carbon, resulting in a less sterically hindered carbanion at the former 4-position. The increased prevalence of dienyl (I) in polyisoprenyl-Li and the increased nucleophilicity of the carbon at the former 4-position may explain the termination reactions in DME only observed for polyisoprenyl-Li.

The amount of 1,4-units increased by 3 − 5% with increasing polymerization temperature from 0 to 23 °C, regardless of the 1,3-diene employed. On the other hand, both the amount of 3,4- and of 1,2-units decrease with increased temperatures. Table 3 gives a comparison of the PI microstructures in various solvents.

Interestingly, PI synthesized in DME exhibits even fewer 1,4-units (≈ 10%) than PI synthesized in THF (≈ 14%).[17] This was unexpected, since generally, more polar solvents lead to a greater reduction in 1,4-units.[34] Accordingly, a comparatively high T_g of 12 °C was obtained for PI synthesized in DME compared to T_g = 3 °C in THF.[17] It is known from the literature that the dependence of T_g on the microstructure decreases with increasing size of the 1,3-diene, i.e., $T_{g,PI} > T_{g,PMyr} > T_{g,PFar}$.[89] Hence, a relatively low value of T_g

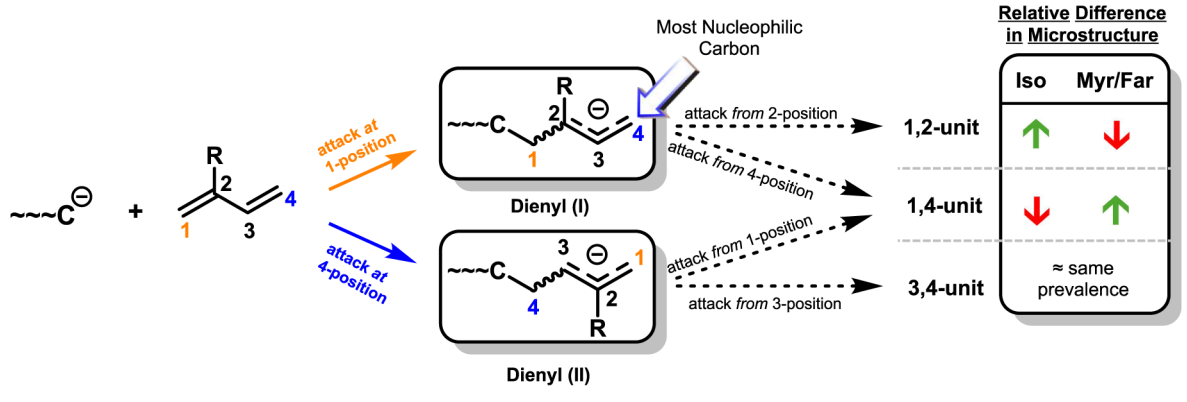

Figure 4. Pathways for the formation of each microstructure. Note: The sum of 1,4- and 4,1-units is summarized as 1,4-units.

https://doi.org/10.1021/acs.macromol.6c01289
Macromolecules 2026, 59, 8274−8284

Table 3. Comparison of Distributions of PI Microstructures in Different Solvents

solvent	T (°C)	1,4-[d] (%)	3,4-[d] (%)	1,2-[d] (%)	T_g[e] (°C)
CHx[a]	RT	95	5	0	−69
MTBE[b]	23	45.7	50.4	3.9	n.d.
THF[a]	RT	14	62	24	3
DME[c]	23	10.3	69.4	20.3	12

[a]Taken from Glatzel et al.[17] [b]Taken from Meier-Merziger et al.[15] [c]Iso3 (Table 1). [d]Determined via ^{1}H NMR spectroscopy. [e]Determined via DSC.

≈ −68 °C was found for PFar in spite of a vinyl content (i.e., sum of 3,4- and 1,2-units), VC, of ≈ 72%, while the T_g of PMyr is ≈ −48 °C. Due to its small side chains and high vinyl content of ≈ 90%, the T_g of PI lies at ≈ 12 °C.

Effect of DME on Kinetics of Styrene Polymerization in Cyclohexane

Small amounts of THF, deliberately added as a "modifier" to polymerizations of styrene in hydrocarbons, are known to dramatically accelerate the reaction, whereas further amounts of added polar solvent lead to a decrease in the reaction rate, finally reaching a level higher than without any added polar solvent.[60] Using in situ NIR kinetic measurements, in this work, the effect of varying CHx/DME solvent mixtures on k_{app} was investigated, while keeping the amount of added initiator with regard to the total reaction volume relatively constant ([P*] = 1.3−1.8 mM). All pseudo first-order plots exhibit a constant slope k_{app}, and the dispersities are $Đ$ = 1.03−1.06 (see Table S2 and Figures S39−S41). Figure 5 shows the obtained k_{app} values in DME/CHx together with published data in THF/benzene.[60]

As for THF, the addition of small amounts of DME to the reaction drastically accelerates the polymerization of styrene. This is explained by the formation of a very reactive monoetherate when small amounts of polar solvents are added, and less reactive dietherates, when more polar solvent is added.[90] The highest value of k_{app}, corresponding to a factor of

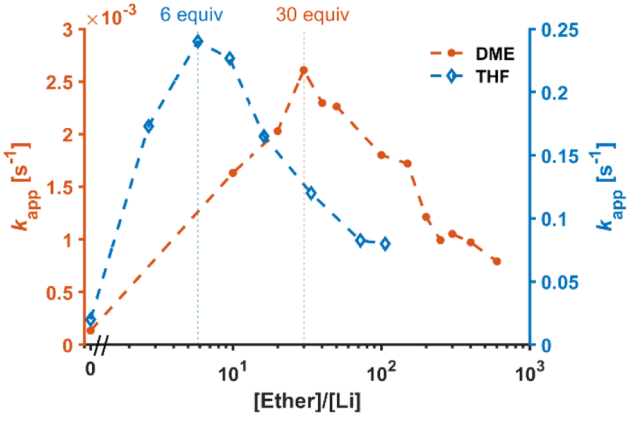

Figure 5. Plot of k_{app} of styrene at 20 °C against the equiv of the respective ether. Left axis: Values for DME determined via NIR kinetics ([P*] = 1.3 − 1.8 mM, solvent: CHx). See Table S2 for the data. Right axis: Published values for THF ([P*] = 0.96 − 1.2 mM, solvent: benzene). The values in THF are reproduced from "Anionic polymerization of styrene effect of tetrahydrofuran", Copyright S. Bywater, D. J. Worsfold[60] (licensed under CC-BY 4.0), https://creativecommons.org/licenses/by/4.0/. The dashed lines are only a guide to the eye. Note the different scales on the y-axes.

acceleration compared to pure CHx, F_{acc}, of ≈ 18, is reached at [DME]/[Li] = 30. At [DME]/[Li] = 600, the increase in k_{app} dropped to F_{acc} ≈ 6. Since anionic polymerizations in aromatic hydrocarbons are faster than in CHx,[63,91,92] the corresponding F_{acc} values for THF cannot be compared with the obtained values for DME. However, the respective equiv of ether required to reach the highest k_{app} values follow the expected trend, i.e., ≈ 6 equiv of the more polar THF compared to ≈ 30 equiv of the less polar DME.

Additionally, it was reported that for styrene polymerizations in benzene, the kinetic order N with respect to the initiator is increased from one-half to one, if 0.15 M THF is present.[60] We found that for 0.08 M DME, the kinetic order for styrene polymerizations in CHx at 20 °C is one (Table S2 and Figure S38). However, this finding does not necessarily mean that DME has a larger effect on N than THF, since there is no published data regarding the effect of THF on N for [THF] < 0.15 M.

Microstructure of PI Synthesized in DME with Various Alkali Naphthalenides

As mentioned above, Scott et al. long ago observed that besides ethyl methyl ether, DME is the only other noncyclic monoether in which Na-Naph is formed quantitatively.[42] Evidently, the dielectric constant renders DME sufficient to promote the electron transfer from alkali metals to naphthalene by solubilizing the alkali ions. Alkali naphthalenide, especially Na-Naph, is a well-known difunctional initiator for anionic polymerizations, typically used in polymerizations in THF at temperatures of −78 °C, affording polymers with narrow molecular weight distributions.[93−96] Generally, it is known from the literature that the use of nonlithium alkali counterions at temperatures of −20 °C and above leads to chain termination reactions and therefore higher dispersities.[97−102] For example, $Đ$ = 1.64 was reported for polybutadiene initiated by sodium naphthalenide at 0 °C in THF.[102]

In this work, isoprene was initiated with Li-, Na-, K-, Rb-, and Cs-Naph in DME at room temperature in a reactor (Figure S19, for experimental details, see Supporting Information, Section 1.6). Dispersities for Na, K, Rb, and Cs between $Đ$ = 1.52 and 2.26 were obtained, whereas a comparatively small value of $Đ$ = 1.13 was achieved when Li-Naph was used as the initiator for isoprene in DME at rt (Table S3, Figure S50). Figure 6 shows the dependence of the different polyisoprene microstructures determined by ^{1}H NMR and of the obtained T_g values on the counterion (Table S3, Figure S49).

With increasing size of the alkali ion, the amount of 1,4-units increases, rising substantially from sodium (12%) to potassium (40%). While the amount of 1,2-units varies little with increasing ionic radius, the amount of 3,4-units decreases, dropping off significantly from sodium (75%) to potassium (44%). Exactly the same trends were found by Salle et al. for isoprene polymerized in 1,4-dioxane at 15 °C using Li-, Na-, K-, and Cs-Naph, as can be seen in Figure S48, which shows a comparison of PI microstructures for different alkali counterions and solvents.[28] The amounts of *cis*- and *trans*-1,4-units (determined using ^{13}C NMR spectroscopy, see Supporting Information, Section 6 for more details) are shown in Figure S47. While for Li and Na the absolute amounts of *cis*- and *trans*-1,4-units are ≈ 4−7% each, for the other alkali metals the fraction of *trans*-1,4-units increases to 29−34%, whereas the increase of *cis*-1,4-units is less drastic (11−14%). As can be

https://doi.org/10.1021/acs.macromol.6c01289
Macromolecules 2026, 59, 8274−8284

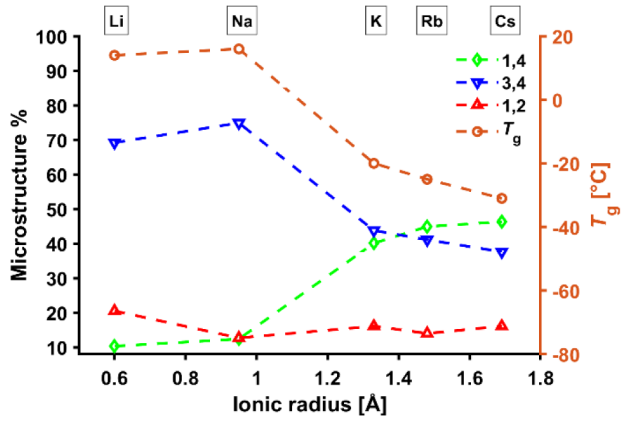

Figure 6. Content of 1,4-, 3,4-, and 1,2-units in PI synthesized in DME at room temperature and glass transition temperature (T_g) against radii of respective alkali counterions. The dashed lines are only a guide to the eye. See Table S3 for the data.

seen in Figure 6, the T_g values correlate well with the vinyl content,[89] being T_g = 14 °C for VC = 90% (Li) and decreasing to T_g = −31 °C for VC = 54% for Cs (Figure S49). Hence, the possibility to quantitatively obtain alkali naphthalenides in DME provides easy access to PI exhibiting different microstructures and glass transition temperatures depending on the counterion. Additional data are provided in Table S3 and Figures S44−S50.

Influence of DME on Copolymerization of Styrene and Isoprene in Cyclohexane

Recently, our group investigated the influence of THF and MTBE as modifiers in S/I copolymerizations regarding reactivity ratios, microstructures, and T_gs.[15,77] We observed that at [THF]/[Li] ≈ 6 and [MTBE]/[Li] ≈ 166, the rate of consumption of both comonomers was equally fast, leading to random incorporation of the comonomers.

In this work, the effect of increasing amounts of DME on S/I copolymerizations in CHx was investigated using the method of in situ NIR kinetics.[103] Information regarding the experimental procedure is given in the Supporting Information, Section 1.5. The studies were conducted at $[sec\text{-BuLi}]_0$ ≈ 1.7 mM up to a ratio of [DME]/[Li] = 450 ([DME] ≈ 770 mM). Further investigations at even higher equiv of DME were not conducted due to the lack of a pressure-resistant NIR setup. Figures S51−S52 show the individual time-conversion plots. To avoid overfitting, the ideal, nonterminal model (r_I r_S = 1, Jaacks fit) was used to determine the reactivity ratios for [DME]/[Li] ≥ 20, whereas the terminal model (Meyer-Lowry fit) was used when the linear Jaacks fit failed.[104−107] All kinetic data and polymer characteristics of the conducted S/I copolymerizations are given in Table 4, and more information can be found in the Supporting Information, Section 8.

The time to reach 50% conversion of the initial individual monomer concentration, $t_{1/2}$, of both monomers decreases up to [DME]/[Li] = 240, with styrene exhibiting a stronger decline of $t_{1/2}$ (Figure S57). Interestingly, an increase to [DME]/[Li] = 450 raises $t_{1/2}$ for both monomers. This was also observed for the polar modifiers THF (minimum of $t_{1/2}$ at [THF]/[Li] ≈ 80) and for MTBE (minimum of $t_{1/2}$ at [MTBE]/[Li] ≈ 1000).[15,77] Here again, the equivalents required for the lowest $t_{1/2}$ value follow the polarity of the solvent, i.e., MTBE < DME < THF. Although, as shown above, for the homopolymerization of styrene the highest rate of monomer consumption is reached at ≈ 30 equiv DME, this cannot be applied to copolymerizations with isoprene due to the occurrence of crossover effects.

Starting at highly preferred isoprene incorporation at [DME]/[Li] = 0 (r_I = 9.91, r_S = 0.007), leading to a tapered copolymer architecture, the reactivity ratios steadily converge until [DME]/[Li] ≈ 40, where both monomers are incorporated randomly (r_I ≈ r_S ≈ 1). Random incorporation of monomers is also evidenced by the minimum of sequences of at least three consecutive styrene units ("blockiness", Figure 7a) in the S/I copolymer.[108,109] Noteworthily, the point of inversion of S/I reactivity in DME, THF, and MTBE correlates with polarity, i.e., the more polar the modifier is the less amount is needed to reach the point of inversion. Accordingly, the inversion of the S/I reactivity ratios is more pronounced for [DME]/[Li] = 450 (r_S = 2.50, r_I = 0.40) than for a similar copolymerization conducted in pure MTBE (r_S = 1.82, r_I = 0.55), corroborating the stronger modifier effect of DME compared to MTBE.[15] Similarly, the vinyl content at [DME]/

Table 4. Overview of Polymer Characteristics of All Synthesized S/I Copolymers in DME at 20 °C

[DME]/[Li]	M_n^{SEC}[a] (kg mol^{-1})	$Đ$[a]	r_I	r_S	$r_I \cdot r_S$	*cis*-1,4-[b] (%)	*trans*-1,4-[b] (%)	3,4-[c] (%)	1,2-[c] (%)	T_g[d] (°C)	Molar Gradient
0	72.4	1.09	9.91	0.007	0.07	66.5	29.8	3.7	0	-38/99	PI PS
2	96.9	1.08	3.01	0.06	0.18	45.0	38.9	15.6	0.5	-11/99	PI PS
8	81.2	1.06	1.19	0.22	0.26	29.4	43.7	25.2	1.7	19	PI PS
20	77.1	1.07	1.32	0.76	1	25.4	41.0	30.9	2.7	25	PI PS
40	84.9	1.08	0.96	1.04	1	24.9	37.3	34.3	3.5	25	PI PS
80	100.2	1.07	0.78	1.28	1	23.8	31.4	40.8	4.0	31	PI PS
120	100.0	1.09	0.69	1.44	1	22.8	28.8	43.8	4.6	30	PI PS
240	81.3	1.09	0.60	1.67	1	22.0	23.3	49.2	5.5	33	PI PS
450	91.4	1.07	0.40	2.50	1	19.2	19.5	52.2	9.1	40	PI PS

[a]Determined by SEC (calibration: PS, eluent: THF). [b]Determined by ^{13}C NMR. [c]Determined by ^{1}H NMR. [d]Determined by DSC (heating rate: 10 K/min). For SEC and DSC results, see Figures S55−S56.

https://doi.org/10.1021/acs.macromol.6c01289
Macromolecules 2026, 59, 8274−8284

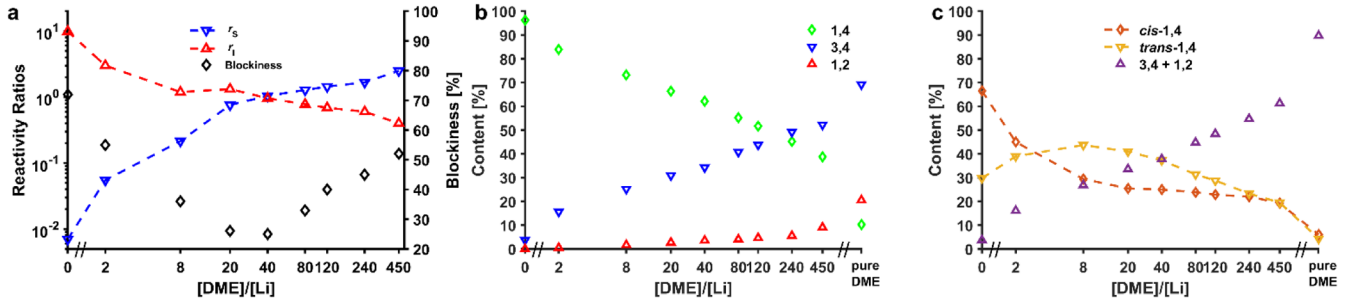

Figure 7. (a) Effect of [DME]/[Li] on the reactivity ratios and on the occurrence of -SSS- triad sequences ("blockiness") in the S/I copolymer. (b) Effect of [DME]/[Li] on occurrence of 1,4-, 3,4-, and 1,2-units in the S/I copolymer. (c) Effect of [DME]/[Li] on occurrence of *cis*- and *trans*-1,4-units and the sum of 3,4- and 1,2-units (vinyl content) in the S/I copolymer.

[Li] = 450 (≈ 61%, Figure 6b,c) already exceeds the vinyl content of S/I copolymers in pure MTBE (≈ 54%).[15] Interestingly, although the overall content of 1,4-units decreases with increasing equiv of DME, the *trans*-1,4-units initially increase from 29.8% in pure CHx to 43.7% for 8 equiv DME, after which they steadily decrease to 4.3% in pure DME (Figure 7c).

CONCLUSIONS

To the best of our knowledge, this is the first comprehensive investigation of the anionic polymerization of isoprene, myrcene, farnesene, and styrene using dimethyl ether as a solvent or cosolvent of intermediate polarity. First, using in situ ^{1}H NMR spectroscopy the half-life of the degradation of *n*-BuLi in DME was measured as $t_{1/2}^{DME} \approx 280$ min, whereas in MTBE, studied in a previous work, the half-life of *n*-BuLi was about one order of magnitude higher with $t_{1/2}^{MTBE} \approx 2600$ min.[15] In the subsequent investigation, all investigated 1,3-dienes showed kinetic orders of unity, indicating (i) the presence of unaggregated unimeric polydienyl-Li chain ends and (ii) the absence of an equilibrium between polydienyl-Li ion pairs and free polydienyl anions in DME. This enabled the determination of their absolute rate constants and their activation energies of chain propagation. The effect of DME on S/I copolymerizations in CHx was also investigated. Following the polarity of the solvent, (i) the polymerization rate constant and (ii) activation energy of polyisoprenyl-Li in DME, (iii) the stability of *n*-BuLi in DME, and (iv) the influence of DME on S/I copolymerizations in CHx was found to be in between the more polar THF and the less polar MTBE.

In contrast to MTBE and CHx, isoprene polymerized faster in DME than *β*-farnesene. Interestingly, the polymerization of both myrcene and farnesene exhibited comparable activation energies and microstructures, whereas isoprene showed a significantly lower activation energy and a distinct microstructure. Additionally, first-order chain termination reactions were observed for polymerizations of isoprene but not for myrcene and farnesene. While for homopolymerizations of styrene in benzene only ≈6 equiv of THF are required for the maximum polymerization rate, at comparable chain end concentrations in CHx 30 equiv of DME are needed for the largest increase in monomer consumption. Since, in pronounced contrast to MTBE, the synthesis of alkali naphthalenides as difunctional initiators is feasible in DME, isoprene was successfully polymerized using the naphthalenides of Li, Na, K, Rb, and Cs. Surprisingly, the polymerization of isoprene in DME with Li as a counterion leads to polyisoprene with a higher vinyl content (≈ 90%) than in the more polar THF, exhibiting T_g values of up to 13 °C, which is desirable for postpolymerization modification reactions.

Although DME requires special handling due to its low boiling point, its production on a megaton scale, its nontoxicity, easy evaporation and recovery, and particularly the absence of peroxide formation render it suitable as an alternative solvent for anionic polymerization of styrene and 1,3-dienes.

ASSOCIATED CONTENT

Supporting Information

The Supporting Information is available free of charge at https://pubs.acs.org/doi/10.1021/acs.macromol.6c01289.

Detailed experimental description, instrumentation, kinetics of *n*-BuLi decomposition in DME, homopolymerization kinetics of isoprene, myrcene, and *β*-farnesene in DME, S/I copolymerization kinetics, determination of chain concentrations, termination constants, reactivity ratios, microstructures, and blockiness, NMR spectra of homo- and copolymers, SEC and DSC curves (PDF)

AUTHOR INFORMATION

Corresponding Authors

Holger Frey − *Johannes Gutenberg-University of Mainz, Department of Chemistry, Mainz 55128, Germany;* orcid.org/0000-0002-9916-3103; Email: hfrey@uni-mainz.de

Axel H. E. Müller − *Johannes Gutenberg-University of Mainz, Department of Chemistry, Mainz 55128, Germany;* orcid.org/0000-0001-9423-9829; Email: muellax@uni-mainz.de

Authors

Frédéric S. Petrov − *Johannes Gutenberg-University of Mainz, Department of Chemistry, Mainz 55128, Germany*

Manfred Wagner − *Max Planck Institute for Polymer Research, Mainz 55128, Germany*

Complete contact information is available at: https://pubs.acs.org/10.1021/acs.macromol.6c01289

Author Contributions

F.S.P., H.F., and A.H.E.M. conceptualized the article. All synthetic work was conducted by F.S.P. The setup of the NMR

https://doi.org/10.1021/acs.macromol.6c01289
Macromolecules 2026, 59, 8274−8284

spectrometer for ^{1}H NMR kinetic experiments was performed by M.W. The manuscript was primarily written by F.S.P. and complemented by H.F., and A.H.E.M. All authors have given approval to the final version of the manuscript.

Notes

The authors declare no competing financial interest.

■ ACKNOWLEDGMENTS

We thank Amyris for providing β-farnesene.

■ ABBREVIATIONS

DME, dimethyl ether; THF, tetrahydrofuran; NIR, near-infrared; CHx, cyclohexane; MTBE, methyl *tert*-butyl ether; k_p, propagation rate constant; k_{app}, apparent propagation rate constant; k_t, termination constant; E_A, activation energy; $[P^*]$, concentration of polymer chains; $[M]_0$, initial monomer concentration; M_M, monomer molecular weight; M_n, number average molecular weight; SEC, size exclusion chromatography; DSC, differential scanning calorimetry; T_g, glass transition temperature; NMR, nuclear magnetic resonance; VC, vinyl content; RT, room temperature; S, styrene; I, isoprene; Myr, Myrcene; Far, Farnesene; r, reactivity ratio

■ REFERENCES

(1) Steube, M.; Johann, T.; Barent, R. D.; Müller, A. H.; Frey, H. Rational design of tapered multiblock copolymers for thermoplastic elastomers. *Prog. Polym. Sci.* **2022**, *124*, 101488.
(2) Steube, M.; Johann, T.; Plank, M.; Tjaberings, S.; Gröschel, A. H.; Gallei, M.; Frey, H.; Müller, A. H. E. Kinetics of Anionic Living Copolymerization of Isoprene and Styrene Using in Situ NIR Spectroscopy: Temperature Effects on Monomer Sequence and Morphology. *Macromolecules* **2019**, *52* (23), 9299−9310.
(3) Wahlen, C.; Blankenburg, J.; Tiedemann, P. V.; Ewald, J.; Sajkiewicz, P.; Müller, A. H. E.; Floudas, G.; Frey, H. Tapered Multiblock Copolymers Based on Farnesene and Styrene: Impact of Biobased Polydiene Architectures on Material Properties. *Macromolecules* **2020**, *53* (23), 10397−10408.
(4) Grune, E.; Johann, T.; Appold, M.; Wahlen, C.; Blankenburg, J.; Leibig, D.; Müller, A. H. E.; Gallei, M.; Frey, H. One-Step Block Copolymer Synthesis versus Sequential Monomer Addition: A Fundamental Study Reveals That One Methyl Group Makes a Difference. *Macromolecules* **2018**, *51* (9), 3527−3537.
(5) Rösler, A.; Weidner, S. M.; Klamroth, T.; Müller, A. H. E.; Schlaad, H. Kinetics of anionic polymerization of β-myrcene in hydrocarbon solvents*Polym. Int.***2025**
(6) Tobolsky, A. V.; Rogers, C. E. Anionic polymerization of isoprene: Effect of ionic character of the growing ion pair on polymer structure. *J. Polym. Sci.* **1959**, *38* (133), 205−207.
(7) Tobolsky, A. V.; Rogers, C. E. Isoprene polymerization by organometallic compounds. II. *J. Polym. Sci.* **1959**, *40* (136), 73−89.
(8) Bywater, S.; Firat, Y.; Black, P. E. Microstructures of polybutadienes prepared by anionic polymerization in polar solvents. Ion-pair and solvent effects. *J. Polym. Sci. Polym. Chem. Ed.* **1984**, *22* (3), 669−672.
(9) Geacintov, C.; Smid, J.; Szwarc, M. Kinetics of Anionic Polymerization of Styrene in Tetrahydrofuran. *J. Am. Chem. Soc* **1962**, *84* (13), 2508−2514.
(10) Carvajal, C.; Tölle, K. J.; Smid, J.; Szwarc, M. Studies of Solvation Phenomena of Ions and Ion Pairs in Dimethoxyethane and Tetrahydrofuran. *J. Am. Chem. Soc.* **1965**, *87* (24), 5548−5553.
(11) Bhattacharyya, D. N.; Lee, C. L.; Smid, J.; Szwarc, M. The absolute rate constants of anionic propagation by free ions and ion-pairs of living polystyrene. *Polymer* **1964**, *5*, 54−56.
(12) Dainton, F. S.; Harpell, G. A.; Ivin, K. J. Kinetics of anionic polymerization of α-methyl-styrene in tetrahydrofuran and dioxane. *Eur. Polym. J.* **1969**, *5* (3), 395−403.
(13) Dainton, F. S.; East, G. C.; Harpell, G. A.; Hurworth, N. R.; Ivin, K. J.; Laflair, R. T.; Pallen, R. H.; Hui, K. M. The Kinetics of Anionic Polymerization of Styrene and α-Methylstyrene. Effects of Counter-ion and Solvent. *Makromol. Chem.* **1965**, *89* (1), 257−262.
(14) Meier-Merziger, M.; Imschweiler, J.; Hartmann, F.; Niebuur, B.-J.; Kraus, T.; Gallei, M.; Frey, H. Bifunctional Carbanionic Synthesis of Fully Bio-Based Triblock Structures Derived from β-Farnesene and ll-Dilactide: Thermoplastic Elastomers. *Angew. Chem., Int. Ed.* **2023**, *62* (42), No. e202310519.
(15) Meier-Merziger, M.; Fuchs, D. A. H.; Frey, H.; Müller, A. H. E. Spotlight on Methyl tert-Butyl Ether—Underrated or Overlooked? Unveiling Its Role for Living Anionic Polymerization. *Macromolecules* **2024**, 8154−8161.
(16) Meier-Merziger, M.; Fotaras, N.; Tzourtzouklis, I.; Allouch, C.; Wagner, M.; Müller, A. H. E.; Floudas, G.; Frey, H. One-step Synthesis of Fully Biobased Two-Sided Tapered ABA-type Thermoplastic Elastomers. *ACS Sustainable Chem. Eng.* **2024**, *12*, 9922−9933.
(17) Glatzel, J.; Noack, S.; Schanzenbach, D.; Schlaad, H. Anionic polymerization of dienes in 'green' solvents. *Polym. Int.* **2021**, *70* (2), 181−184.
(18) Natori, I.; Natori, S.; Taehee, J.; Ogino, K. The last challenge for living anionic polymerization of 1,3-cyclohexadiene with the s-butyllithium/cyclopentyl methyl ether system. *Polymer* **2022**, *250*, 124821.
(19) Han, X.; Yang, Y.; Long, Y.; Chen, Z.; Wang, Y.; Dai, Q.; Yi, W.; Li, L.; Liu, K. Highly efficient and quantitative epoxidation of the Poly(1,3-pentadiene) with controlled microstructure synthesized by living anionic polymerization. *Polymer* **2025**, *338*, 129036.
(20) Fu, Y.; Yang, S.; Xiong, Q.; Gu, Z.; Dai, Q.; Tan, H.; Zhou, L.; Geng, M.; Xie, F.; Yi, W.; Li, L.; Liu, K. Synthesis, kinetic study and characterization of C5-dienes/styrene copolymers via living anionic polymerization in cyclopentyl methyl ether solvent. *Polym. Int.* **2024**, *73*, 326−336.
(21) Schmitt, B. J.; Schulz, G. V. The influence of polar solvents on ions and ion pairs in the anionic polymerization of styrene. *Eur. Polym. J.* **1975**, *11* (2), 119−130.
(22) Dyball, C. J.; Worsfold, D. J.; Bywater, S. Anionic Polymerization of Isoprene in Diethyl Ether. *Macromolecules* **1979**, *12* (5), 819−822.
(23) Böhm, L. L.; Schulz, G. V. Über die elementarprozesse bei der anionischen polymerisation des styrols in tetrahydropyran (THP). *Makromol. Chem.* **1972**, *153* (1), 5−20.
(24) Dainton, F. S.; Ivin, K. J.; Laflair, R. T. Kinetics of anionic polymerization of styrene in tetrahydropyran. *Eur. Polym. J.* **1969**, *5* (3), 379−386.
(25) Morton, M.; McGrath, J. E.; Juliano, P. C. Structure-Property Relationships for Styrene-Diene Thermoplastic Elastomers. *J. Polym. Sci., C Polym. Symp.* **1969**, *26* (1), 99−115.
(26) Geerts, J.; van Beylen, M.; Smets, G. Anionic Polymerization of o- and p-Methoxystyrene. *J. Polym. Sci., Part A: Polym. Chem.* **1969**, *7* (10), 2859−2873.
(27) Ambrose, R. J.; Hergenrother, W. L. Structure of Anionic Poly(2-phenylbutadiene). *Macromolecules* **1972**, *5* (3), 275−279.
(28) Salle, R.; Essel, A.; Gole, J.; Pham, Q.-T. Polymérisation anionique des Diènes. III. Etude thermodynamique de la Propagation du Butadiène et de l'Isoprène par les organo-alcalins. *J. Polym. Sci. Polym. Chem. Ed.* **1975**, *13* (8), 1855−1867.
(29) Komiyama, V. J.; Böhm, L. L.; Schulz, G. V. Kinetik der anionischen Polymerisation von Styrol in Dioxan mit Polystyryl-Natrium als Reaktionträger. *Makromol. Chem.* **1971**, *148* (1), 297−304.
(30) Kraft, R.; Müller, A. H. E.; Höcker, H.; Schulz, G. V. Kinetics of the Anionic Polymerization of Methyl Methacrylate in 1,2-Dimethoxyethane. *Makromol. Chem., Rapid Commun.* **1980**, *1* (6), 363−368.
(31) Shimomura, T.; Smid, J.; Szwarc, M. Reactivities of contact and solvent-separated ion pairs. Anionic polymerization of styrene in dimethoxyethane. *J. Am. Chem. Soc.* **1967**, *89* (23), 5743−5749.

(32) Takaya, K.; Tatsuta, H.; Ise, N. Anionic polymerization of styrene in triglyme-benzene mixtures. *Polymer* **1974**, *15* (10), 631−634.
(33) Dai, Q.; Fu, Y.; Tan, H.; Zhang, Y.; Yang, Y.; Xu, J.; Yi, W.; Tan, R.; Liu, K.; Li, L.; Yang, Z. Living anionic copolymerization of 1,3-pentadiene isomers with alpha-methylstyrene in the presence of 2,2-di(2-tetrahydrofuryl)propane. *Polymer* **2024**, *312*, 127629.
(34) Fuchs, D. A. H.; Hübner, H.; Kraus, T.; Niebuur, B.-J.; Gallei, M.; Frey, H.; Müller, A. H. E. The effect of THF and the chelating modifier DTHFP on the copolymerisation of β-myrcene and styrene: kinetics, microstructures, morphologies, and mechanical properties. *Polym. Chem.* **2021**, *12* (32), 4632−4642.
(35) Müller, M.; Hübsch, U. Dimethyl Ether. In *Ullmann's Encyclopedia Of Industrial Chem.*; Wiley-VCH Verlag GmbH & Co. KGaA, 2000, pp.305−308. DOI:
(36) Wu, J.; Liu, Z.; Pan, J.; Zhao, X. Vapor Pressure Measurements of Dimethyl Ether from (233 to 399) K. *J. Chem. Eng. Data* **2004**, *49* (1), 32−34.
(37) Ziegler, K.; Gellert, H.-G., XVII. Reaktionen zwischen Lithium-alkylen und Äthern. *Justus Liebigs Ann. Chem.* **1950**, *567* (1), 185−195.
(38) Subratti, A.; Lalgee, L. J.; Jalsa, N. K. Liquified dimethyl ether (DME): A green solvent for the extraction of hemp (Cannabis sativa L.) seed oil. *Sustainable Chem. Pharm.* **2019**, *12*, 100144.
(39) Bauer, M. C.; Kruse, A. The use of dimethyl ether as an organic extraction solvent for biomass applications in future biorefineries: A user-oriented review. *Fuel* **2019**, *254*, 115703.
(40) Sorenson, S. C.; Mikkelsen, S.-E. Performance and Emissions of a 0.273 Liter Direct Injection Diesel Engine Fuelled with Neat Dimethyl Ether. *SAE Technol. Pap. Ser.* **1995**, *104*, 80.
(41) Fleisch, T.; McCarthy, C.; Basu, A.; Udovich, C.; Charbonneau, P.; Slodowske, W.; Mikkelsen, S.-E.; McCandless, J. A New Clean Diesel Technology: Demonstration of ULEV Emissions on a Navistar Diesel Engine Fueled with Dimethyl Ether. *SAE Technol. Pap. Ser.* **1995**, *104*, 42.
(42) Scott, N. D.; Walker, J. F.; Hansley, V. L. Sodium Naphthalene. I. A New Method for the Preparation of Addition Compounds of Alkali Metals and Polycyclic Aromatic Hydrocarbons. *J. Am. Chem. Soc.* **1936**, *58* (12), 2442−2444.
(43) Subratti, A.; Lalgee, L. J.; Jalsa, N. K. Liquefied dimethyl ether (DME) as a green solvent in chemical reactions: Synthesis of O -alkyl trichloroacetimidates. *Sustainable Chem. Pharm.* **2018**, *9*, 46−50.
(44) Oh, K. S.; Bae, W.; Cho, D. W.; Lee, Y.-W.; Kim, H. Dispersion polymerization of NVCA in compressed liquid dimethyl ether in the presence of PDMS-g-pyrrolidone carboxylic acid: Effects of initiators. *Korean J. Chem. Eng.* **2008**, *25* (4), 854−860.
(45) Oh, K. S.; Bae, W.; Kim, H. Dispersion polymerization of N-vinylcarbazole using siloxane-based and fluorine-based surfactants in compressed liquid dimethyl ether. *Polymer* **2007**, *48* (6), 1450−1454.
(46) Oh, K. S.; Bae, W.; Kim, H. Dispersion polymerization of 2-hydroxyethyl methacrylate (HEMA) using siloxane-based surfactant in supercritical carbon dioxide and in compressed liquid dimethyl ether. *Eur. Polym. J.* **2008**, *44* (2), 415−425.
(47) Bibi, G.; Jung, Y.; Lim, J. C.; Kim, S. H. A Faster Approach to Stereocomplex Formation of High Molecular Weight Polylactide Using Supercritical Dimethyl Ether. *Polymer Korea* **2015**, *39* (3), 453−460.
(48) Bibi, G.; Jung, Y.; Lim, J.-C.; Kim, S. H. Novel Strategy of Lactide Polymerization Leading to Stereocomplex Polylactide Nanoparticles Using Supercritical Fluid Technology. *ACS Sustainable Chem. Eng.* **2016**, *4* (9), 4521−4528.
(49) Cho, D. W.; Oh, K. S.; Bae, W.; Kim, H.; Lee, Y.-W. Synthesis of monodispersed poly(acrylonitrile) microspheres by dispersion polymerization in compressed liquid dimethyl ether. *Colloid Polym. Sci.* **2009**, *287* (2), 179−188.
(50) Hättasch, J.; Schmidt, A.; Strohmann, C. Crystal structure and Hirshfeld surface analysis of lithium chloride and lithium bromide with dimethyl ether ligands. *Acta Crystallogr., Sect. E: Crystallogr. Commun.* **2025**, *81* (Pt11), 1086−1093.
(51) Shatenshtein, A. I.; Petrov, E. S.; Yakovleva, E. A. Effect of solvent and metal on the formation equilibria of naphthalene and diphenyl anion radical. *J. Polym. Sci., C Polym. Symp.* **1967**, *16* (3), 1729−1737.
(52) Holstege, C. P.; Goodrich, W. R. Dimethyl ether. In *Encyclopedia Of Toxicology*; Elsevier, 2024, pp.781−784. DOI:
(53) Dimethyl ether (DME). *Toxicol Ind. Health.* **2022**, *38* (11), 713−716..
(54) Naito, M.; Radcliffe, C.; Wada, Y.; Hoshino, T.; Liu, X.; Arai, M.; Tamura, M. A comparative study on the autoxidation of dimethyl ether (DME) comparison with diethyl ether (DEE) and diisopropyl ether (DIPE). *J. Loss Prev. Process Ind.* **2005**, *18* (4−6), 469−473.
(55) Waller, F. J. *Commercial-scale demonstration of the Liquid Phase Methanol (LPMEOH) Process. Peroxide formation of dimethyl ether in methanol mixtures*; United States Department Of Energy. 1997, .
(56) Hamid, S. H.; Ali, M. A. Effect of MTBE blending on the properties of gasoline. *Fuel Sci. Technol. Int.* **1995**, *13* (5), 509−544.
(57) Loescher, M. E. *Process for the Production of Dimethyl Ether*. US 8,378,150 B2 2013.
(58) Frei, M. S.; Mondelli, C.; García-Muelas, R.; Kley, K. S.; Puértolas, B.; López, N.; Safonova, O. V.; Stewart, J. A.; Curulla Ferré, D.; Pérez-Ramírez, J. Atomic-scale engineering of indium oxide promotion by palladium for methanol production via CO2 hydrogenation. *Nat. Commun.* **2019**, *10* (1), 3377.
(59) Nathrath, P.; Kroll, F.; Karmann, D.; Geißelbrecht, M.; Schühle, P. Methanol production in a sustainable, mild and competitive process: concept launch and analysis. *Green Chem.* **2025**, *27* (30), 9268−9279.
(60) Bywater, S.; Worsfold, D. J. Anionic polymerization of styrene effect of tetrahydrofuran. *Can. J. Chem.* **1962**, *40* (8), 1564−1570.
(61) Geerts, J.; van Beylen, M.; Smets, G. Anionic polymerization of styrene in the presence of different anisoles. *J. Polym. Sci., Part A: Polym. Chem.* **1969**, *7* (10), 2805−2814.
(62) Sinn, V. H.; Lundborg, C.; Onsager, O. T. Kinetik der „Polymerisation" von Isopren und Styrol mit n-Butyllithium als Katalysator. VII. *Makromol. Chem.* **1964**, *70* (1), 222−259.
(63) Worsfold, D. J.; Bywater, S. Anionic polymerization of styrene. *Can. J. Chem.* **1960**, *38* (10), 1891−1900.
(64) Worsfold, D. J.; Bywater, S. Anionic polymerization of isoprene. *Can. J. Chem.* **1964**, *42* (12), 2884−2892.
(65) Morton, M.; Fetters, L. J. Homogeneous anionic polymerization. V. Association phenomena in organolithium polymerization. *J. Polym. Sci. A Gen. Pap.* **1964**, *2* (7), 3311−3326.
(66) Morton, M.; Bostick, E. E.; Livigni, R. A.; Fetters, L. J. Homogeneous anionic polymerization. IV. Kinetics of butadiene and isoprene polymerization with butyllithium. *J. Polym. Sci. A Gen. Pap.* **1963**, *1* (5), 1735−1747.
(67) Morton, M.; Fetters, L. J.; Bostick, E. E. Mechanisms of homogeneous anionic polymerization by alkyllithium initiators. *J. Polym. Sci., C Polym. Symp.* **1963**, *1* (1), 311−323.
(68) Bhattacharyya, D. N.; Smid, J.; Szwarc, M. Alternative Paths in Anionic Propagation of Ion Pairs. Effect of Solvent and Counterion. *J. Phys. Chem.* **1965**, *69* (2), 624−627.
(69) Schorigin, P. Über die Natriumalkyle und über ihre Reaktion mit den Äthern. *Ber. Dtsch. Chem. Ges.* **1910**, *43* (2), 1931−1938.
(70) Wittig, G.; Löhmann, L. Über die kationtrope Isomerisation gewisser Benzyläther bei Einwirkung von Phenyl-lithium. *Justus Liebigs Ann. Chem.* **1942**, *550* (1), 260−268.
(71) Hückel, W.; Bretschneider, H. Über die Spaltung alicyclischer Äther. *J. Prakt. Chem.* **1938**, *151* (2−3), 61−64.
(72) Letsinger, R. L.; Schnizer, A. W.; Bobko, E. Orientation in the Cleavage of 2-Methoxyoctane by Organoalkali Metal Compounds 1. *J. Am. Chem. Soc.* **1951**, *73* (12), 5708−5710.
(73) Gilman, H.; Haubein, A. H.; Hartzfeld, H. The Cleavage of some ethers by organolithium compounds. *J. Org. Chem.* **1954**, *19* (7), 1034−1040.
(74) Lüttringhaus, A.; Sääf, V. G. Über die Methoden zur Spaltung von Phenoläthern. *Angew. Chem.* **1938**, *51* (52), 915−920.

(75) Fitt, J. J.; Gschwend, H. W. Reaction of n-, sec-, and tert-Butyllithium with Dimethoxyethane (DME): A Correction. *J. Org. Chem.* **1984**, *49* (1), 209−210.
(76) Gilman, H.; Gaj, B. J. Preparation and Stability of Some Organolithium Compounds in Tetrahydrofuran. *J. Org. Chem.* **1957**, *22* (10), 1165−1168.
(77) Steube, M.; Johann, T.; Hübner, H.; Koch, M.; Dinh, T.; Gallei, M.; Floudas, G.; Frey, H.; Müller, A. H. E. Tetrahydrofuran: More than a "Randomizer" in the Living Anionic Copolymerization of Styrene and Isoprene: Kinetics, Microstructures, Morphologies, and Mechanical Properties. *Macromolecules* **2020**, *53* (13), 5512−5527.
(78) Haynes, W. M.*CRC Handbook Of Chemistry And Physics*; 96th Ed.; CRC Press, 2015, DOI:
(79) Zhang, H.; Zeng, Z.; Ma, F.; Wu, Q.; Wang, X.; Cheng, S.; Xie, J. Cyclopentylmethyl Ether, a Non-Fluorinated, Weakly Solvating and Wide Temperature Solvent for High-Performance Lithium Metal Battery. *Angew. Chem.* **2023**, *135* (21), No. e202300771.
(80) Marsden, J.; Maass, O. The discontinuity in the dielectric constant of liquids and their saturated vapors at the critical temperature. *Can. J. Res.* **1935**, *13b* (5), 296−307.
(81) Waack, R.; West, P. Aggregation of n-butyllithium in basic solvents. *J. Organomet. Chem.* **1966**, *5* (2), 188−191.
(82) Baskaran, D.; Müller, A. H. E. Anionic vinyl polymerization—50 years after Michael Szwarc. *Prog. Polym. Sci* **2007**, *32* (2), 173−219.
(83) Müller, A. H. Carbanionic Polymerization: Kinetics and Thermodynamics. In *Comprehensive Polymer Science And Supplements*; Elsevier, 1989, pp.387−423. DOI:
(84) Worsfold, D. J.; Bywater, S. Anionic Polymerization of Styrene: Conductivity Measurements. *J. Chem. Soc.* **1960**, *5234*, 5234.
(85) Bywater, S.; Worsfold, D. J. Anionic polymerization of isoprene. Ion and ion-pair contributions to polymerization in tetrahydrofuran. *Can. J. Chem.* **1967**, *45* (16), 1821−1824.
(86) Tiedemann, P. V.; Blankenburg, J.; Maciol, K.; Johann, T.; Müller, A. H. E.; Frey, H. Copolymerization of Isoprene with p -Alkylstyrene Monomers: Disparate Reactivity Ratios and the Shape of the Gradient. *Macromolecules* **2019**, *52* (3), 796−806.
(87) Garton, A.; Chaplin, R. P.; Bywater, S. Anionic polymerization of isoprene in tetrahydrofuran. *Eur. Polym. J.* **1976**, *12* (10), 697−700.
(88) Spach, G.; Levy, M.; Szwarc, M. 59. Spontaneous slow transformations in the "living" polystyrene system. *J. Chem. Soc.* **1962**, 355−361.
(89) Wahlen, C.; Frey, H. Anionic Polymerization of Terpene Monomers: New Options for Bio-Based Thermoplastic Elastomers. *Macromolecules* **2021**, *54* (16), 7323−7336.
(90) Welch, F. J. Polymerization of Styrene by n-Butyllithium. II. Effect of Lewis Acids and Bases. *J. Am. Chem. Soc.* **1960**, *82* (23), 6000−6005.
(91) Hsieh, H. L. Kinetics of polymerization of butadiene, isoprene, and styrene with alkyllithiums. Part I. Rate of polymerization. *J. Polym. Sci. A Gen. Pap.* **1965**, *3* (1), 153−161.
(92) Hsieh, H. L. Effect of lithium alkoxide and hydroxide on polymerization initiated with alkyllithium. *J. Polym. Sci., Part A: Polym. Chem.* **1970**, *8* (2), 533−543.
(93) Szwarc, M.; Levy, M.; Milkovich, R. Polymerization initiated by electron transfer to monomer. A new method of formation of block polymers. *J. Am. Chem. Soc.* **1956**, *78* (11), 2656−2657.
(94) Hirao, A.; Loykulnant, S.; Ishizone, T. Recent advance in living anionic polymerization of functionalized styrene derivatives. *Prog. Polym. Sci.* **2002**, *27* (8), 1399−1471.
(95) Schmitt, V. B. J.; Schulz, G. V. Über zwei Formen des Initiators Na-Naphthalin und die Bestimmung der „lebenden" Kettenenden bei der anionischen Polymerisation. *Makromol. Chem.* **1969**, *121* (1), 184−204.
(96) Bhattacharyya, D. N.; Lee, C. L.; Smid, J.; Szwarc, M. Reactivities and Conductivities of Ions and Ion Pairs in Polymerization Processes. *J. Phys. Chem.* **1965**, *69* (2), 612−623.
(97) Uchida, S.; Togii, K.; Miyai, S.; Goseki, R.; Ishizone, T. Allylidene Monomers: Anionically Polymerizable 1,1-Disubstituted 1,3-Diene Derivatives. *Macromolecules* **2020**, *53* (22), 10107−10116.
(98) Arest-Yakubovich, A. A.; Pakuro, N. I.; Zolotareva, I. V.; Kristal'nyi, E. V.; Basova, R. V. Polymerization of conjugated dienes initiated by soluble organosodium compounds in hydrocarbon solvents. *Polym. Int.* **1995**, *37* (3), 165−169.
(99) Morton, A. A.; Grovenstein, E., XIII. Polymerization A Comparison of the Action of Organosodium Reagents and of the Alfin Catalyst on Styrene 1. *J. Am. Chem. Soc.* **1952**, *74* (21), 5434−5436.
(100) Cheng, T. C.; Halasa, A. F.; Tate, D. P. Microstructure of Polybutadiene Catalyzed by Alkali Metal tert-butoxides and n-Butylsodium. II. *J. Polym. Sci. Polym. Chem. Ed.* **1973**, *11* (1), 253−259.
(101) Cheng, T. C.; Halasa, A. F.; Tate, D. P. Effect of Alkoxides on Chain Termination and Chain Transfer of Sodium-Catalyzed Polybutadiene. *J. Polym. Sci., Part A: polym. Chem.* **1971**, *9* (9), 2493−2502.
(102) Arest-Yakubovich, A. A.; Anosov, V.; Basova, R.; Zolotarev, V.; Izyumnikov, A.; Kristal'nyi, E.; Nakhmanovich, B.; Rogozhkina, Y.; Sidneva, V. Chain transfer reactions and molecular weight characteristics of butadiene polymers prepared under the action of sodium initiators in the presence of electron donors. *Polym. Sci. U.S.S.R.* **1985**, *27* (3), 714−722.
(103) Lanzendörfer, M. G.; Schmalz, H.; Abetz, V.; Müller, A. H. E.Application of FT-NIR Spectroscopy for Monitoring the Kinetics of Living Polymerizations. In *Situ Spectroscopy Of Monomer And Polymer Synthesis*. Puskas, J. E.; Long, T. E.; Storey, R. F.; Shaikh, S.; Simmons, C. L., Springer US; 2003, 67−81. DOI: .
(104) Jaacks, V. Eine neuartige Methode zur Bestimmung von Copolymerisationsparametern. *Angew. Chem.* **1967**, *79* (9), 419.
(105) Jaacks, V. A novel method of determination of reactivity ratios in binary and ternary copolymerizations. *Makromol. Chem.* **1972**, *161* (1), 161−172.
(106) Meyer, V. E.; Lowry, G. G. Integral and differential binary copolymerization equations. *J. Polym. Sci. A Gen. Pap.* **1965**, *3* (8), 2843−2851.
(107) Hawkins, D. M. The problem of overfitting. *J. Chem. Inf. Comput. Sci.* **2004**, *44* (1), 1−12.
(108) Mochel, V. D. Nuclear Magnetic Resonance-Analog Computer Method for "Block Styrene". *Macromolecules* **1969**, *2* (5), 537−540.
(109) Bovey, F. A.; V. D. Tiers, G.; Filipovich, G. Polymer NSR spectroscopy. I. The motion and configuration of polymer chains in solution. *J. Polym. Sci.* **1959**, *38* (133), 73−90.

https://doi.org/10.1021/acs.macromol.6c01289
Macromolecules 2026, 59, 8274−8284